



Figure 5.4 Binocular microscopic picture of Houma mould of tool, showing two different parts of colours. The left side was inner wall. Width of the image = 8 mm

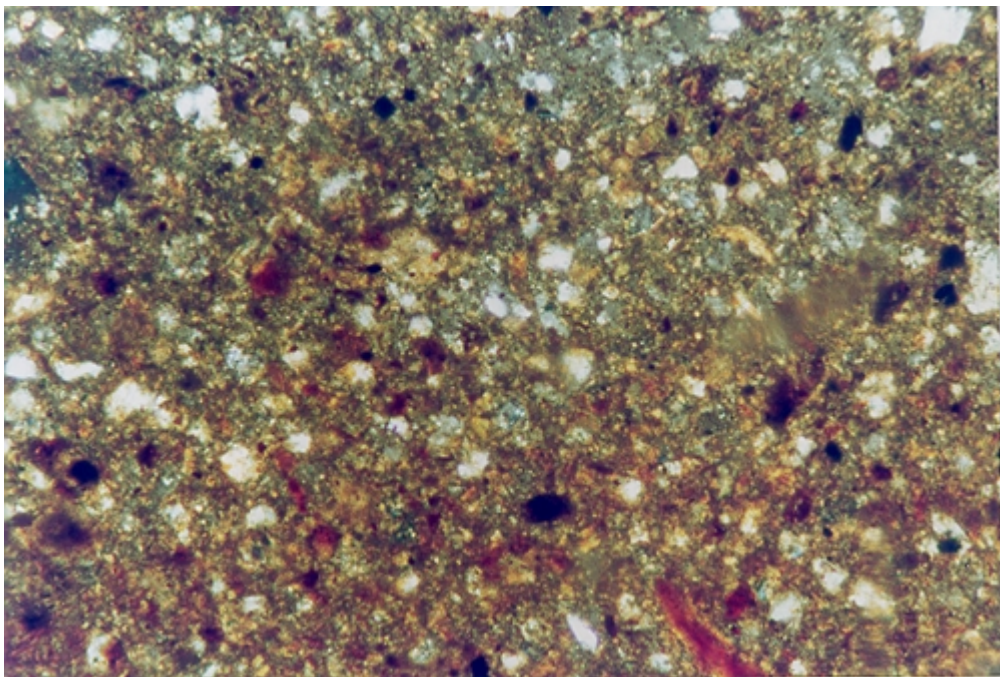


Figure 5.5 Petrographic thin section of Houma mould of tool, showing little difference in texture between grey part (upper half) and brown part. Width of the image = 1 mm



Figure 5.6 Binocular microscopic picture of Houma mould of vessel.
Width of the image = 8 mm

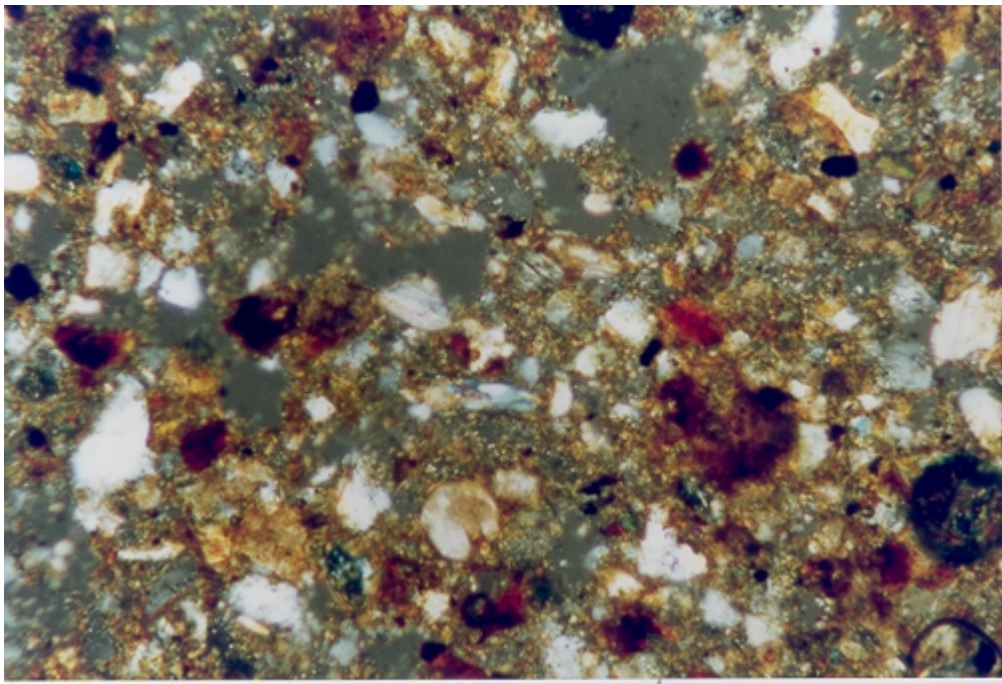


Figure 5.7 Petrographic thin section of Houma mould of vessel
Width of image = 1 mm

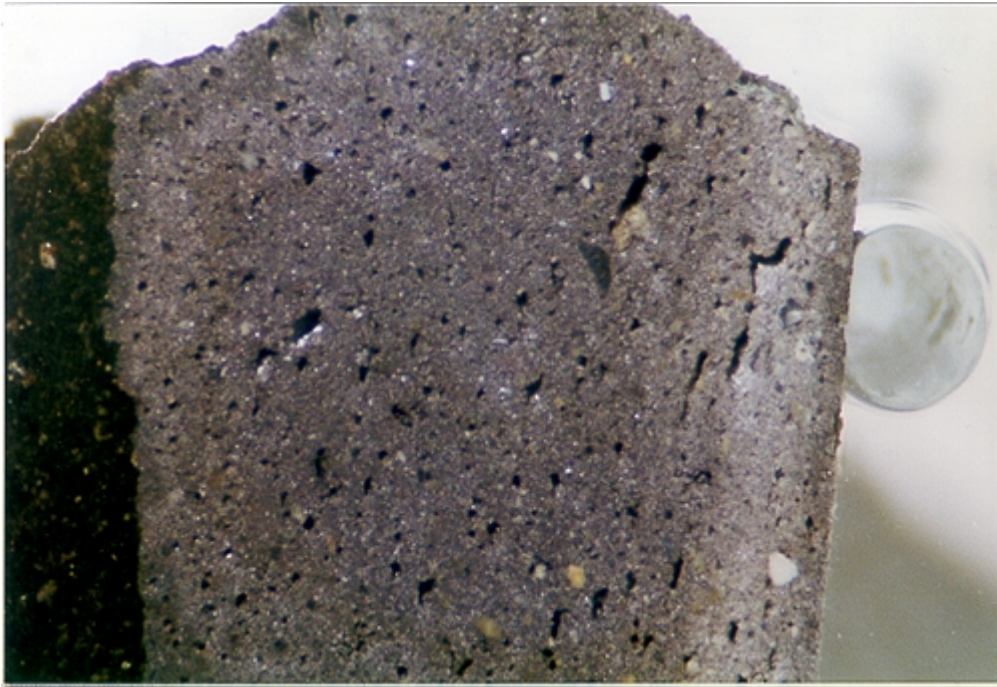


Figure 5.8 Binocular microscopic picture of Western Zhou mould of vessel from Shaanxi, showing two different parts of colours. The right side was inner wall. Width of the image = 8 mm

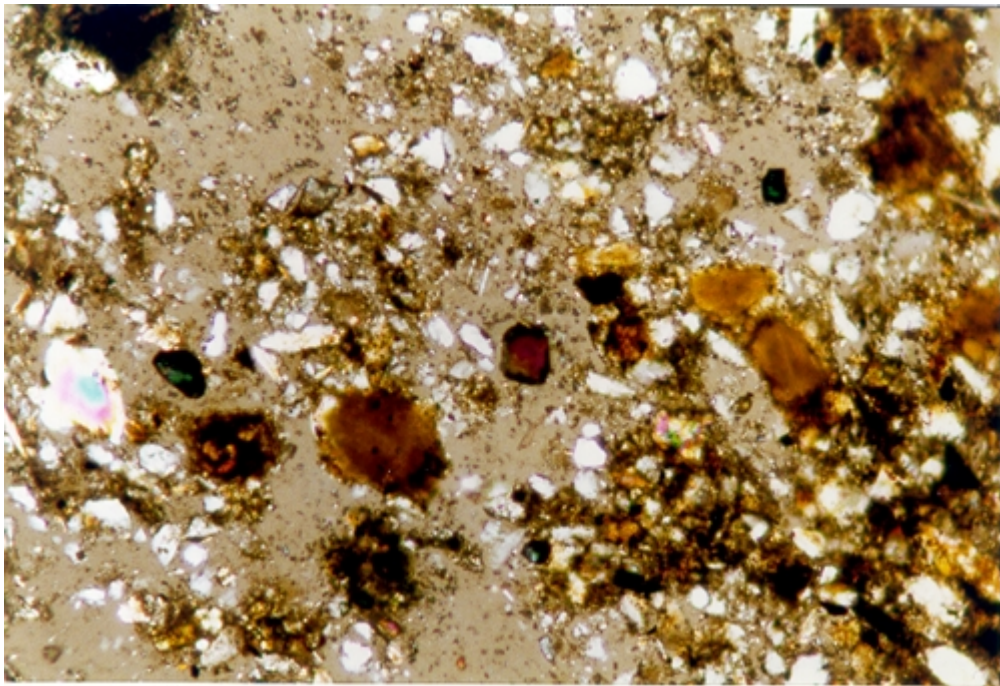


Figure 5.9 Petrographic thin section of Western Zhou mould of vessel from Shaanxi, showing little difference in texture between grey part (upper half) and black part. Width of the image = 1 mm

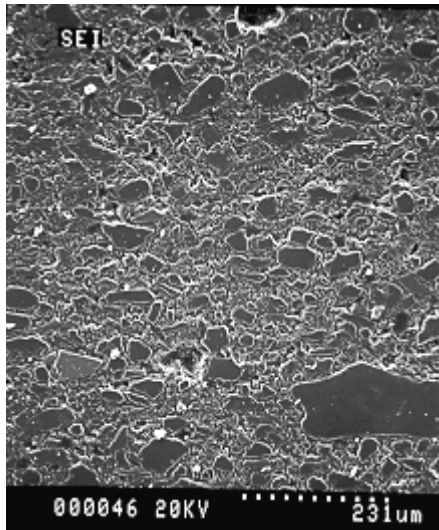


Figure 5.10 SEI of polished section of Houma mould of tool

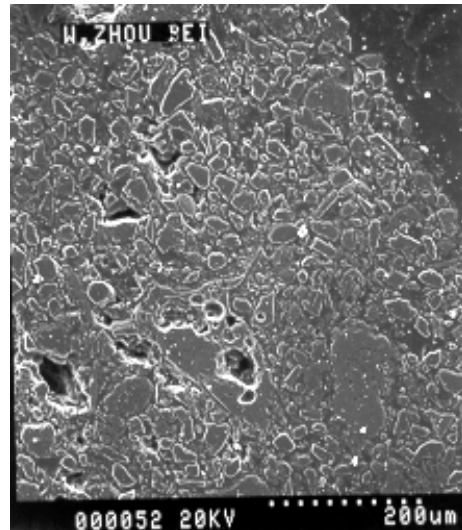


Figure 5.11 SEI of polished section of WZH mould of vessel from Shaanxi

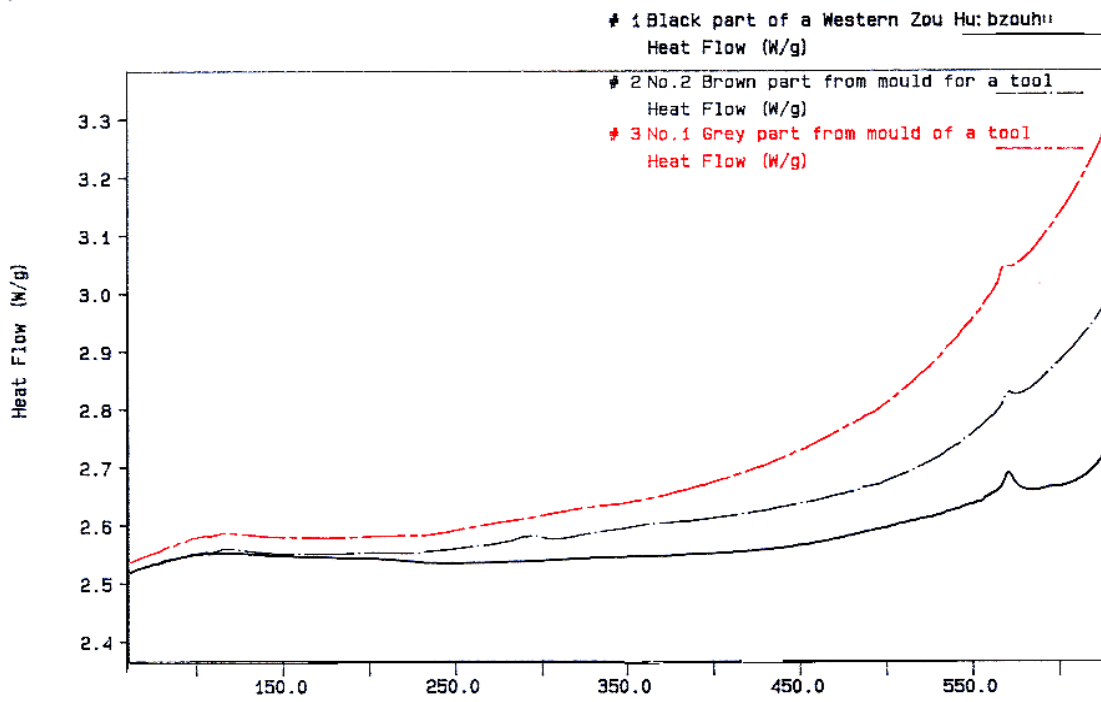


Figure 5.12 Multiplots of DSC curves, showing quartz peak in the moulds

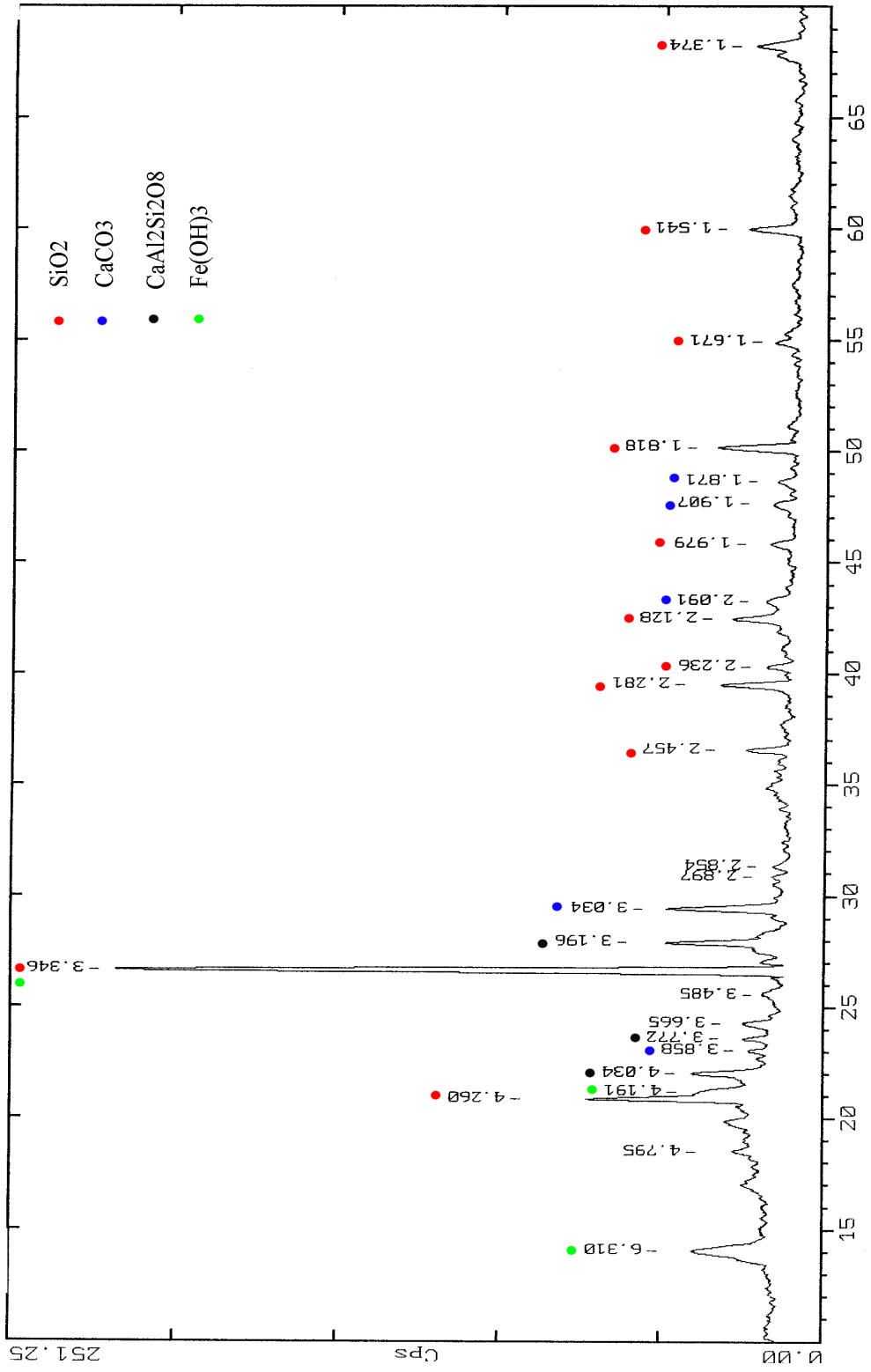


Figure 5.14 XRD spectrum of the mould of Houma vessel

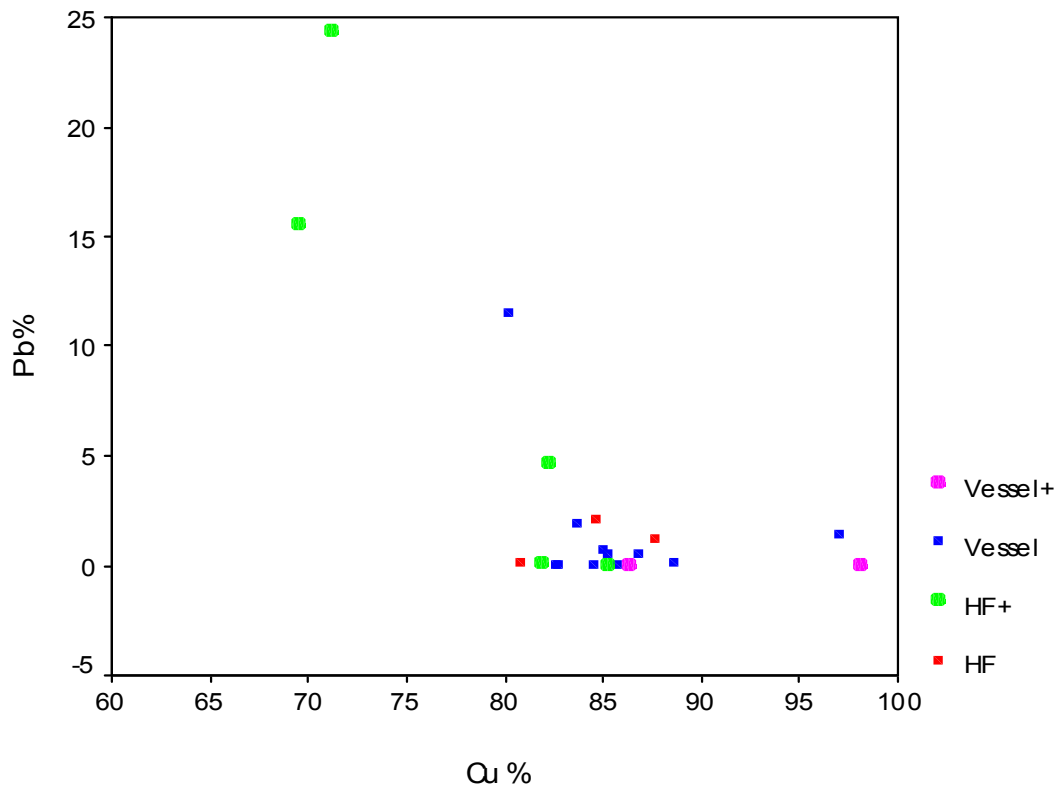
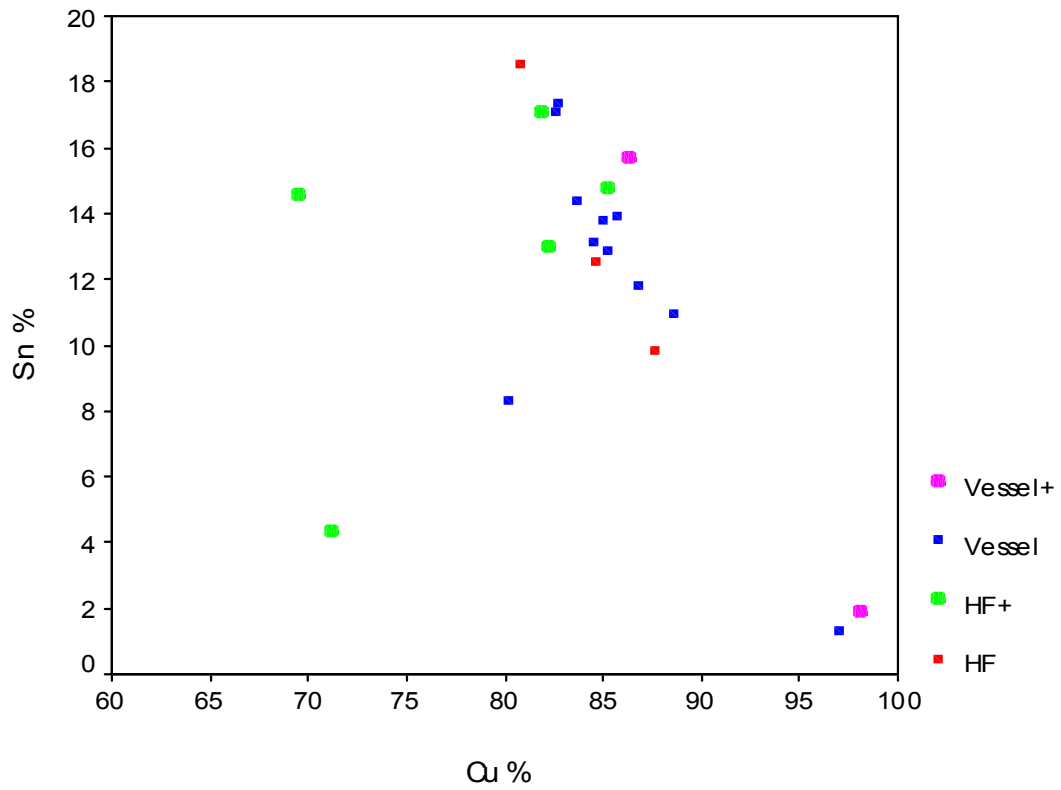


Figure 5.16 Scatterplot for Jin metals, showing more variety in composition for the bronzes from other class tombs (marked with +)

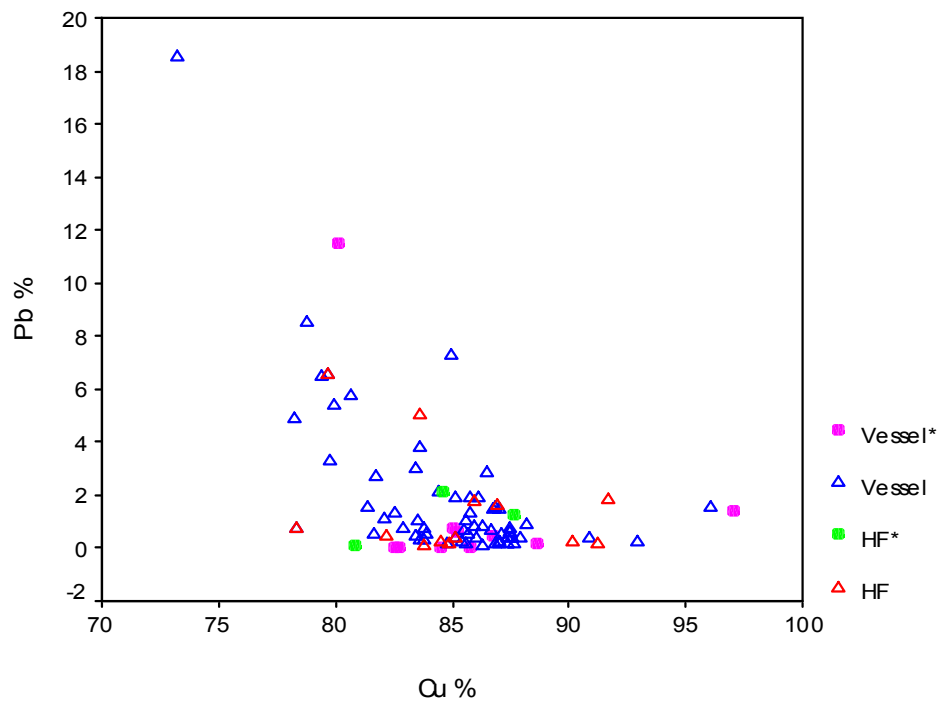
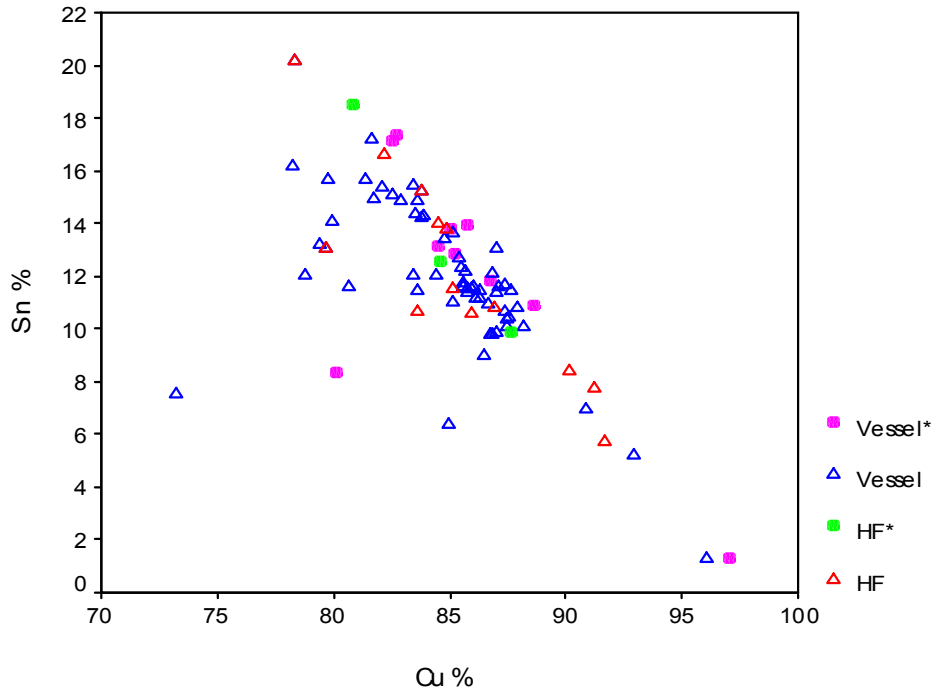


Figure 5.17 Scatterplots for Jin vessels and horse fittings from the elite tombs (AAS data marked with *), showing that AAS and ICP data are comparable. There is little difference in composition of vessels and horse fittings.

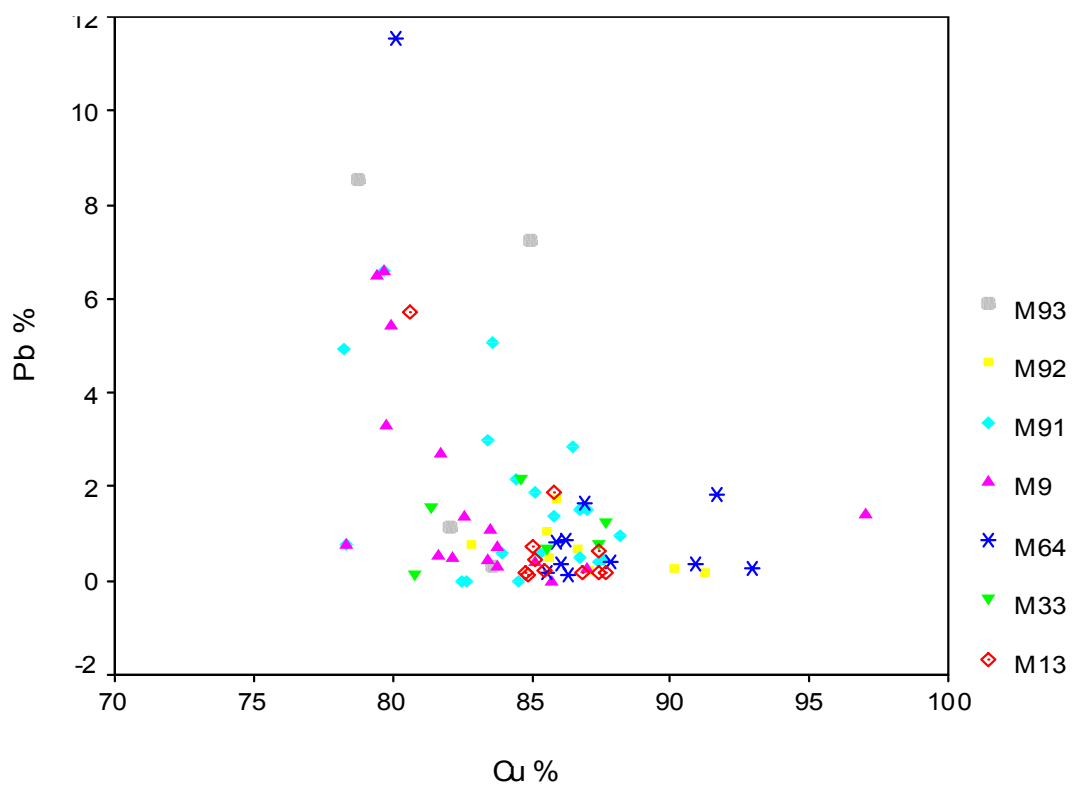
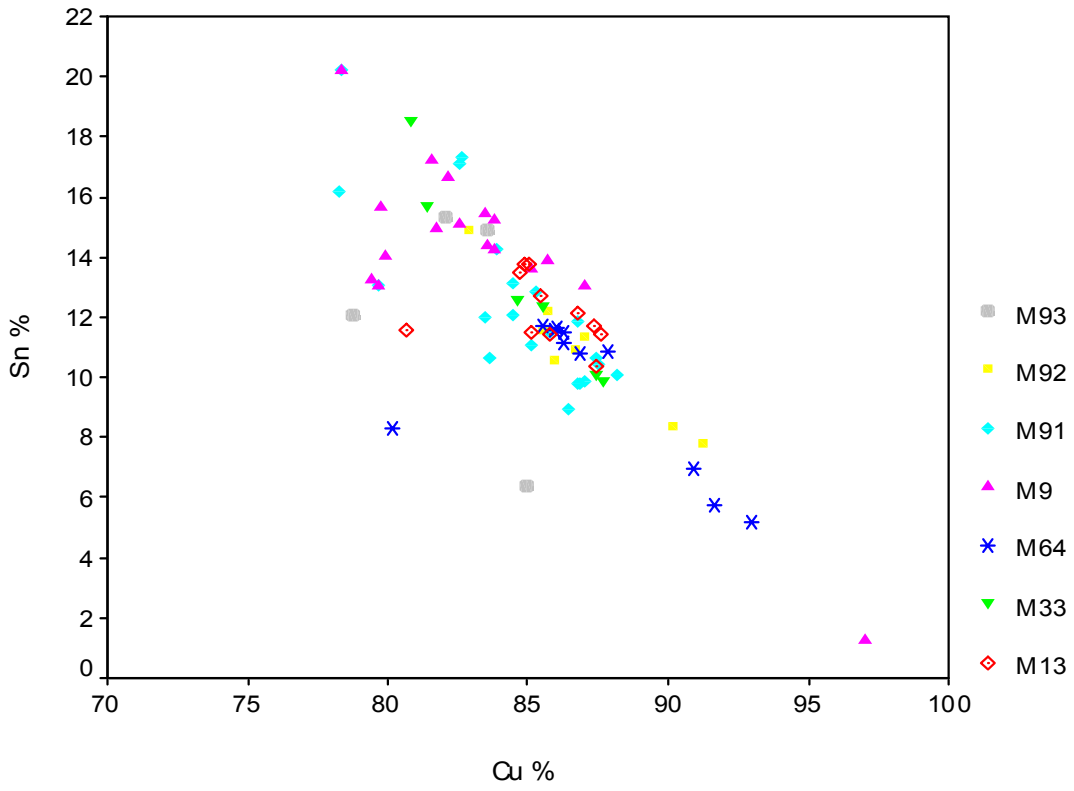


Figure 5.20 Comparison scatterplots for Jin metals (including vessels and horse fittings) from different elite tombs

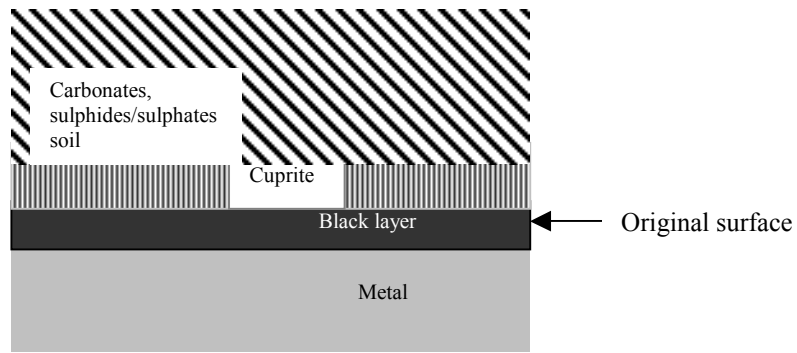
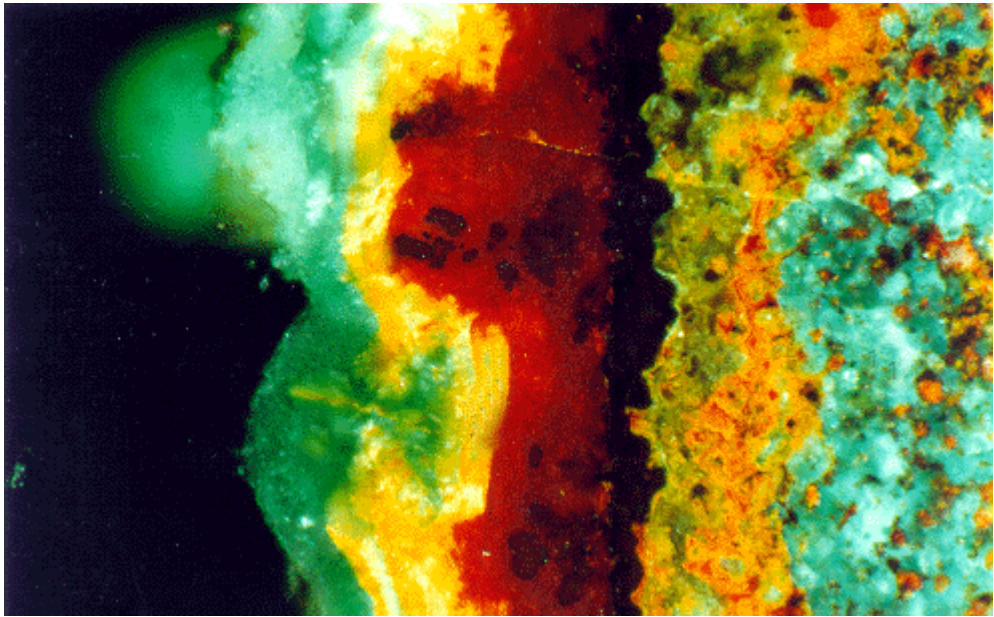
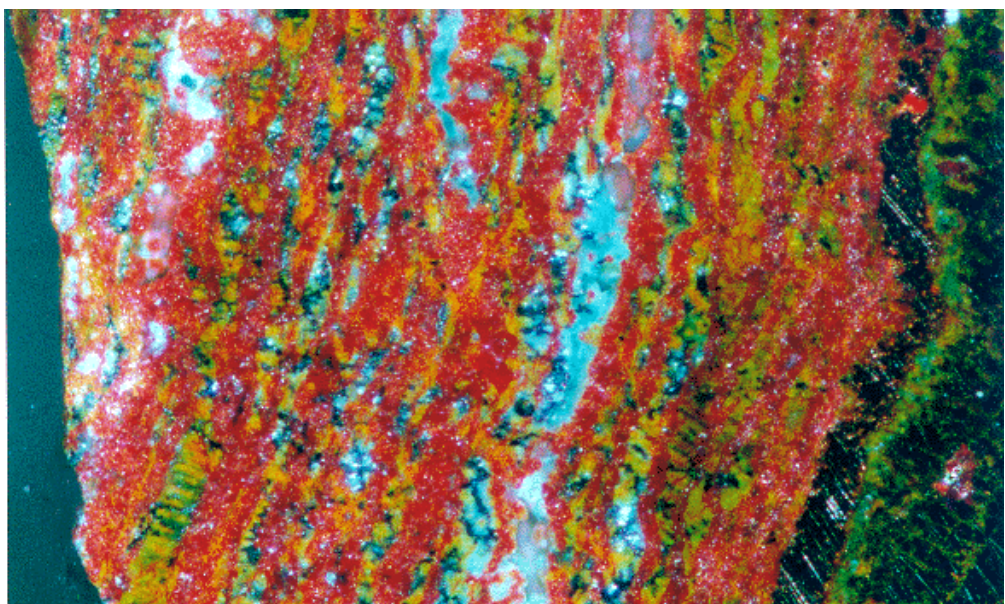


Figure 6.6 Typical surface structure of a corroded Jin bronze



A: Lamellar corrosion (M6231:1. Width of the image = 0.57 mm)



B: Interlaced corrosion (M6384:20. Width of the image = 0.9 mm)

Figure 6.7 Two types of structures of corrosion overburden. Photomicrographs. Cross polarised light.

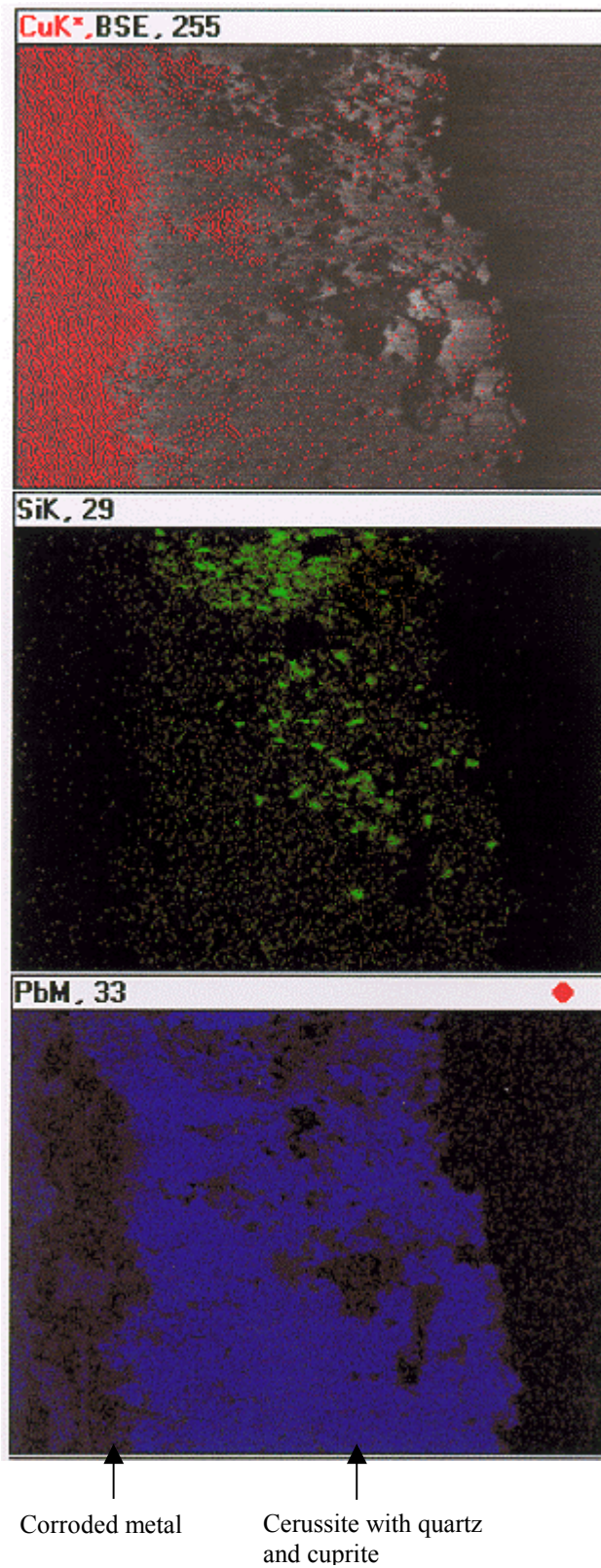


Figure 6.11 SEM/EDS colour maps of lead (mixed with cuprite and quartz grains) in the corrosion overburden of M64:148. 100x

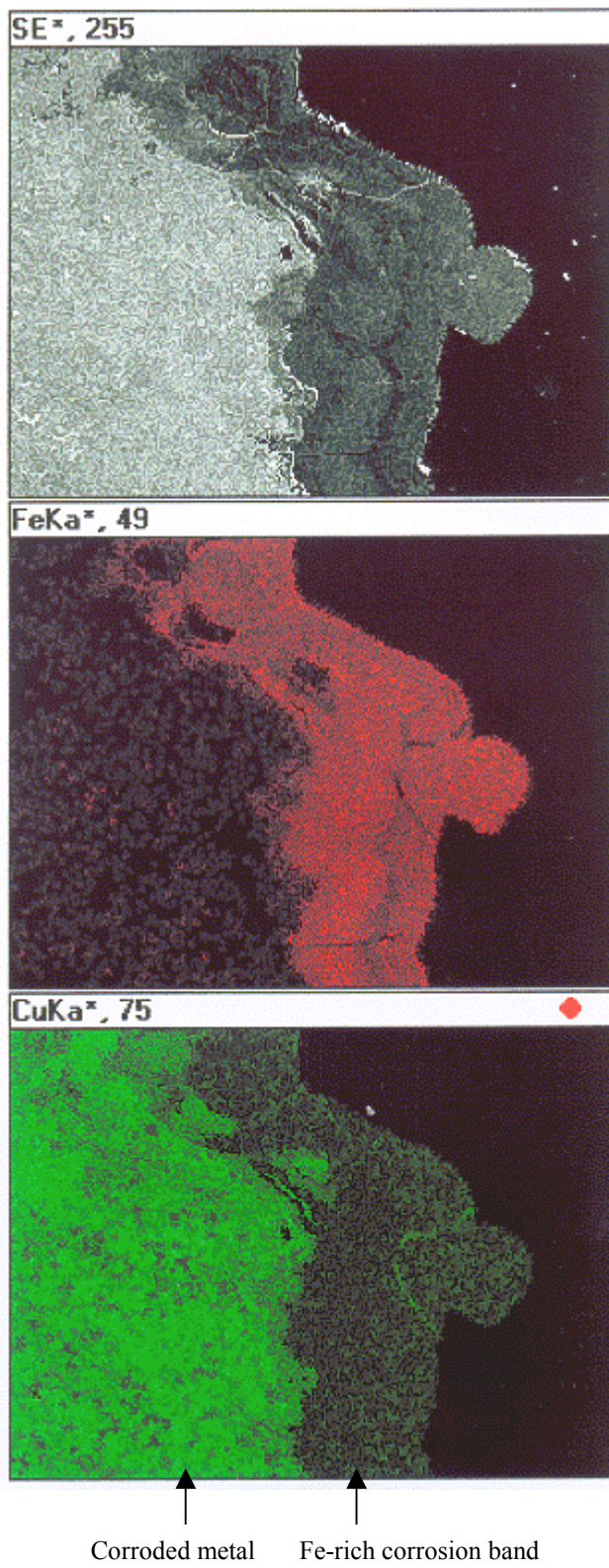


Figure 6.13 SEM/EDS colour maps of Fe-rich corrosion layer on M91:137A. 100x

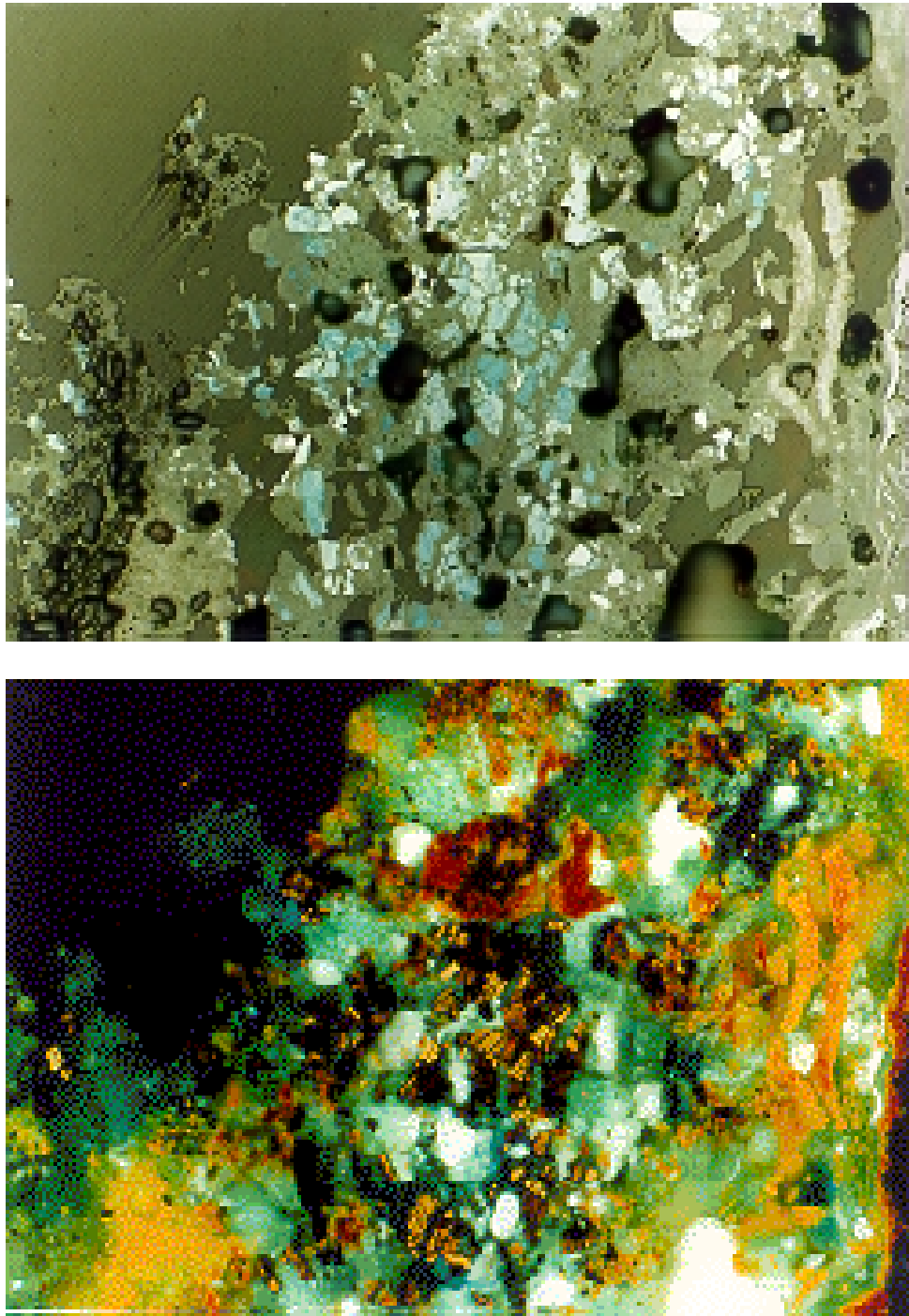
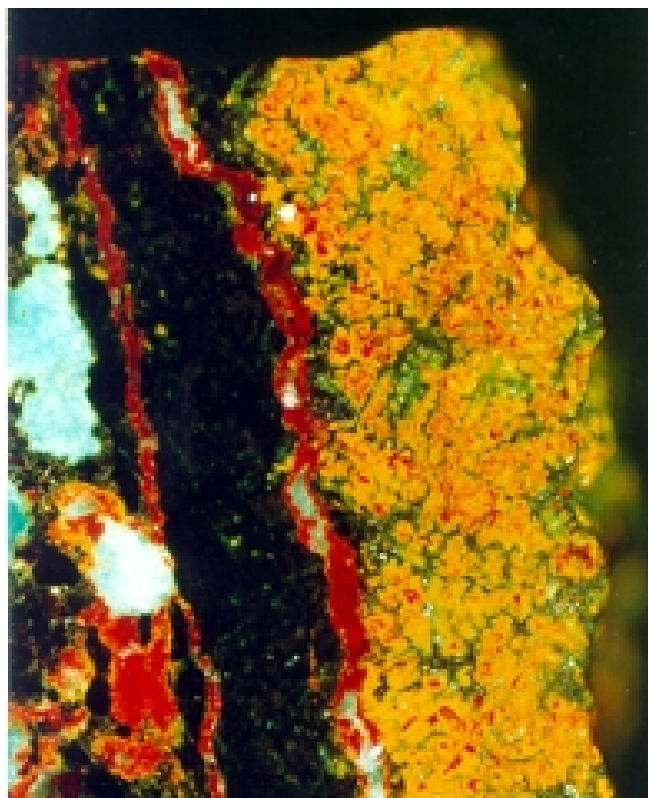


Figure 6.14 Photomicrograph of crystalline copper sulphides with fractures in the corrosion overburden on M91:506A.
Width of the image = 0.7 mm. Top: BF; Bottom: C/P



↑ ↑ ↑
 Corrosion overburden Black layer Corroded metal

M33:unknown1, C/P.
 Height of the image = 1.4 mm



↑ ↑ ↑
 Corrosion overburden Black layer Corroded metal

M6231:74, C/P.
 Height of the image = 0.9 mm

Figure 6.15 Two types of black layers on the Jin bronzes from Tianma-Qucun
 Left: black layer next to the metal Right: black layer within cuprite

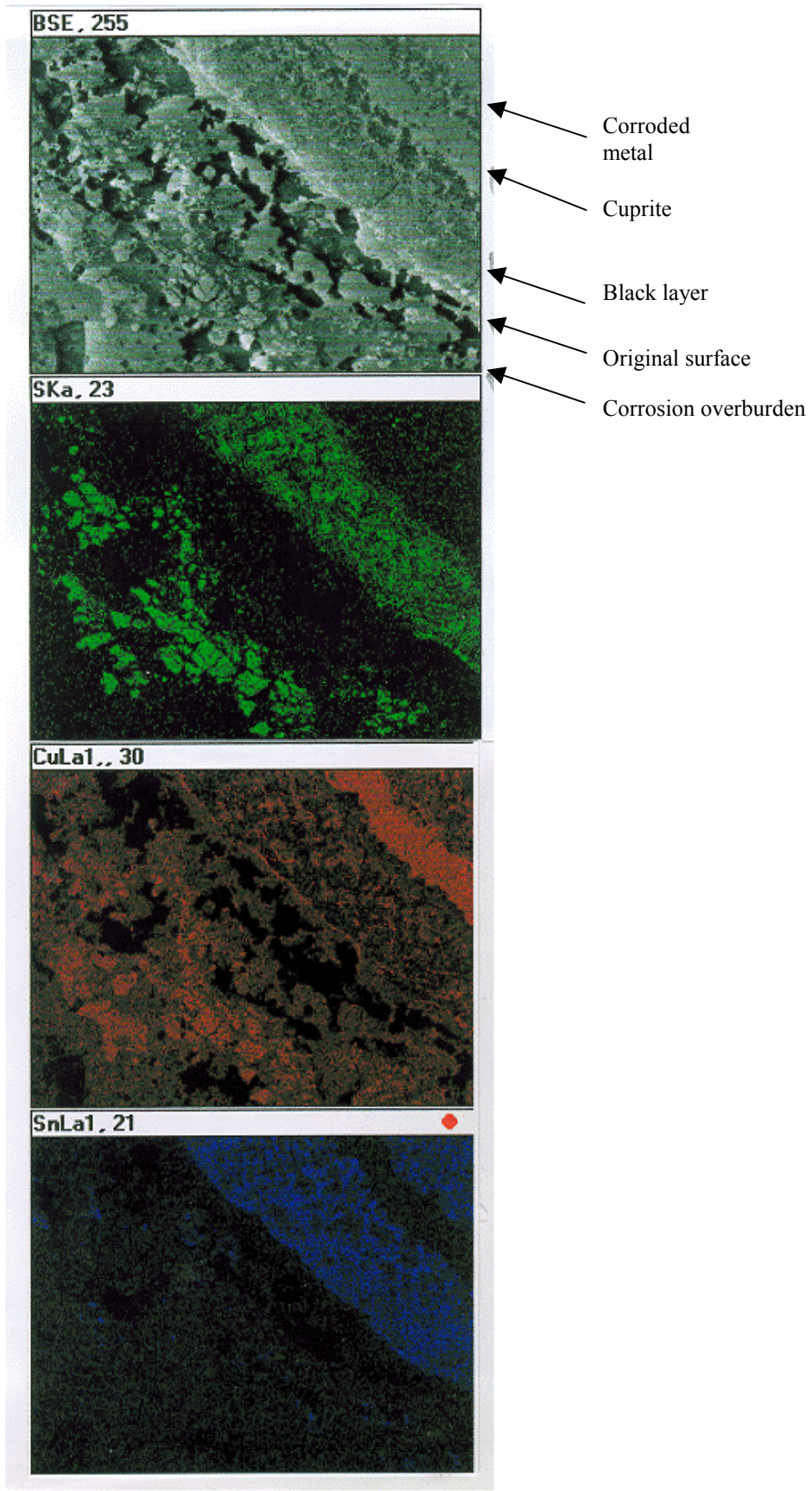
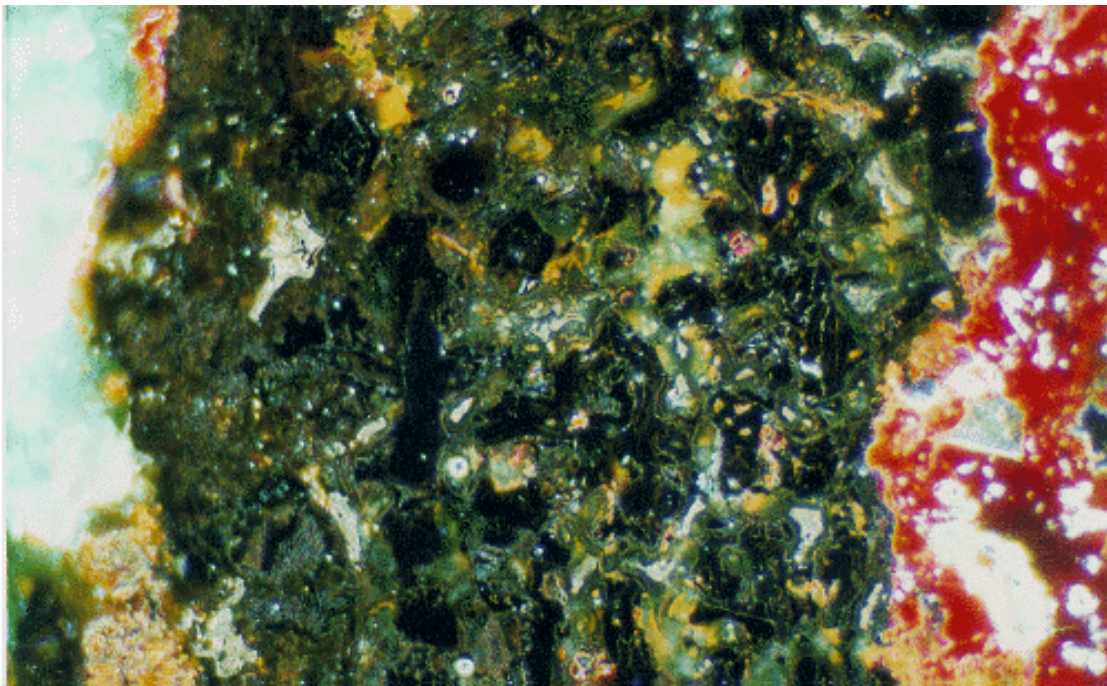
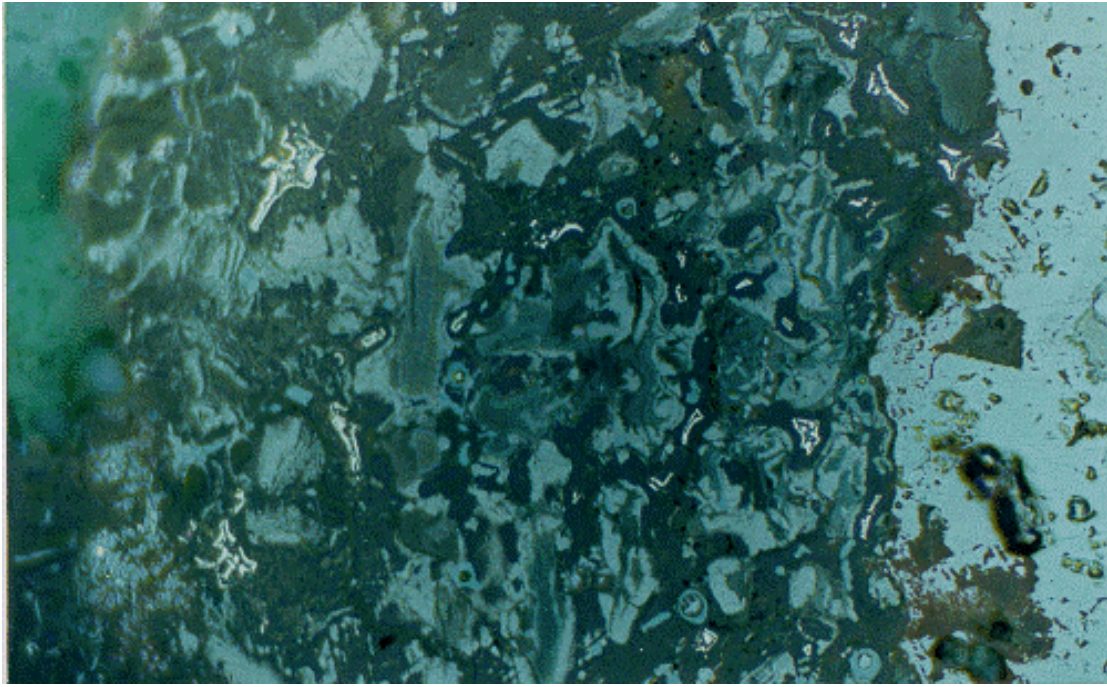


Figure 6.16 SEM/EDS colour maps of corrosion on the surface of M91:506A, showing enrichment of sulphur in the black layer and corrosion overburden. 100x.



Carbonates

Black layer

Cuprite

Figure 6.17 Photomicrograph of the black layer on M91:506A, showing pseudomorphic structure of the original alloy.

Top: BF. Bottom: C/P. Width of the image = 0.2 mm.

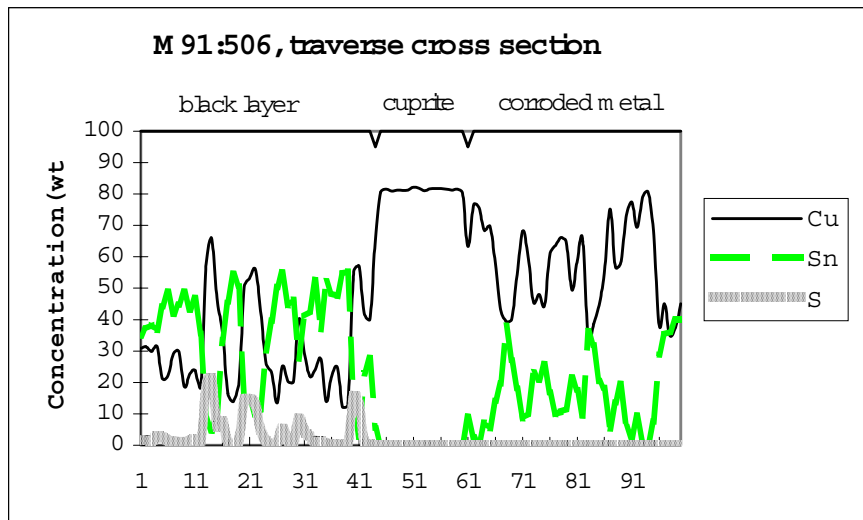


Figure 6.18 EPMA linescans traversing the metallographic section of M91:506A, showing a correlation between Cu & S in the black layer.

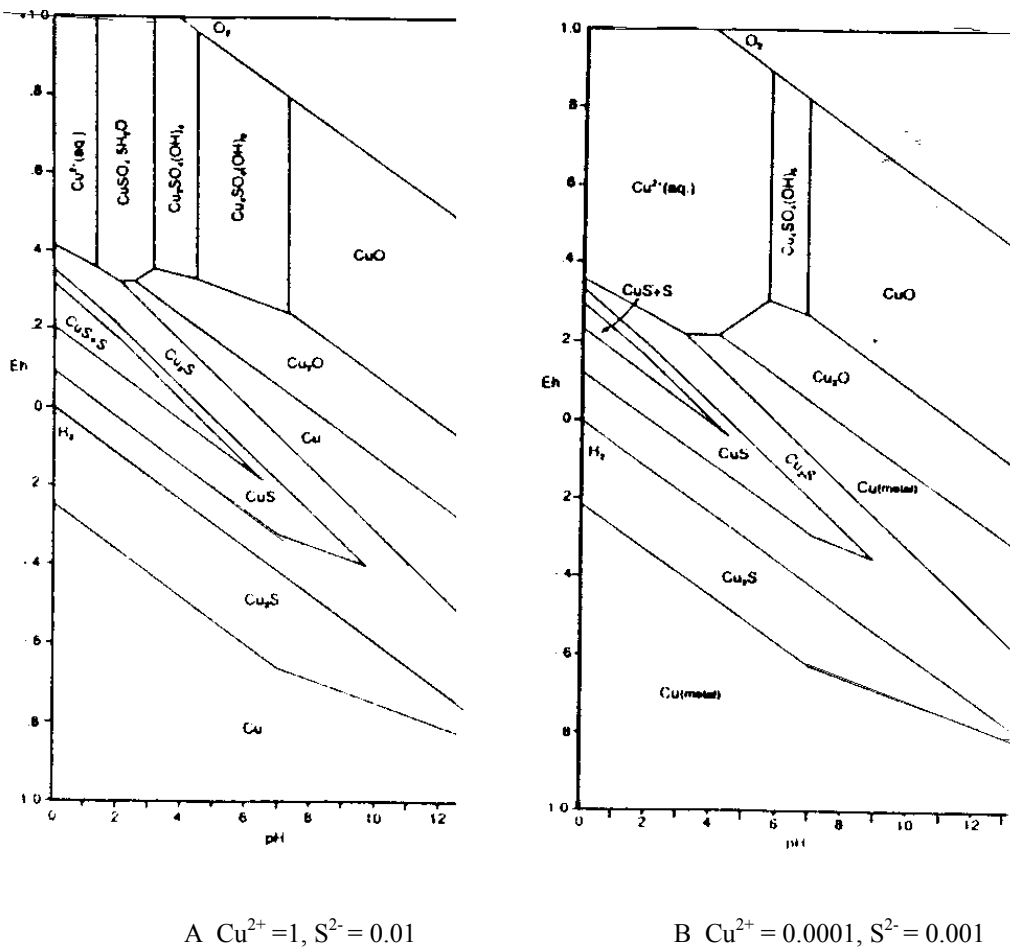
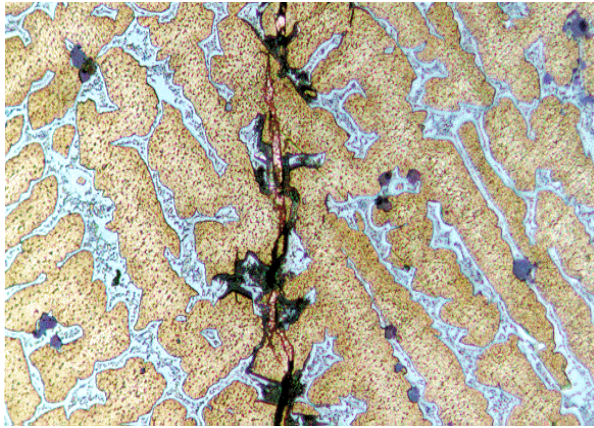
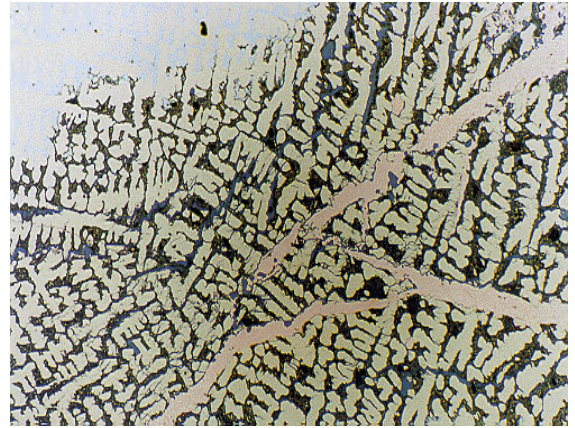


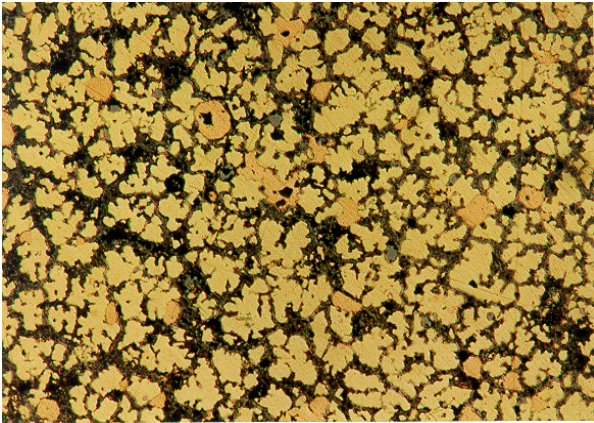
Figure 6.19 Pourbaix diagram of Cu-H-O-S system (After McNeil & Mohr, 1992,1050)



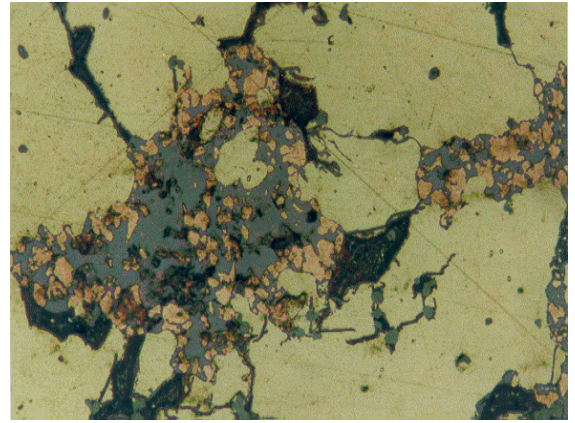
a. Crack filling (M91:400, W = 0.2 mm)



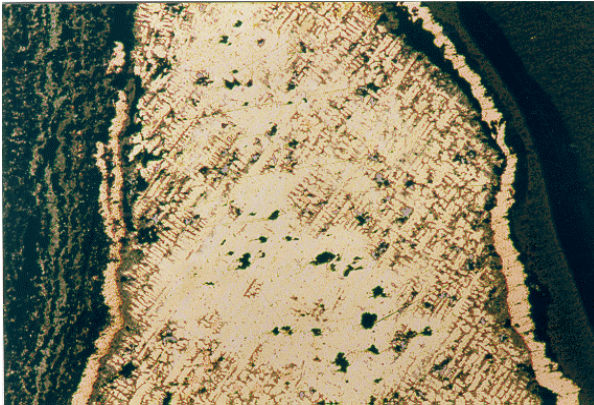
b. In δ -removal area (M33:unknown2, W = 0.7mm)



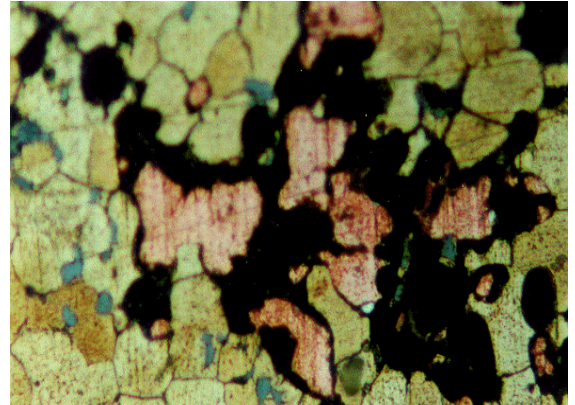
c. Globules in δ -removal area δ (M63:81, W = 1 mm)



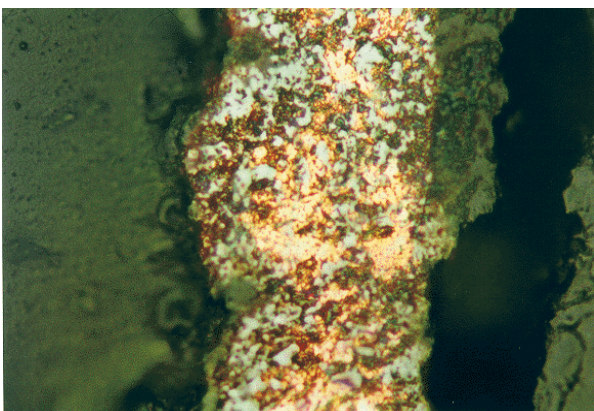
d. Within cuprite in the metal (M13:102, W = 0.2 mm)



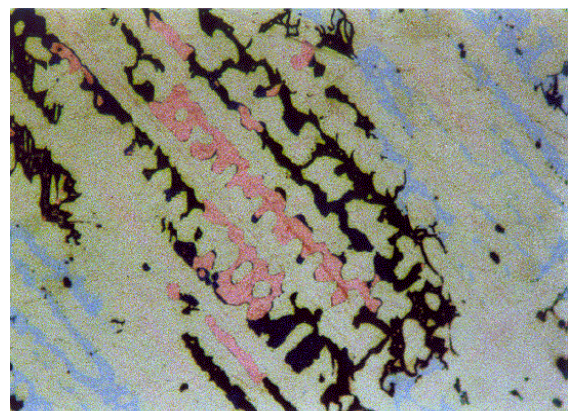
e. Bands on the surface (M6384:20, W = 2 mm)



f. In corrosion pits (M91:140, W = 0.2 mm)



g. Within cuprite at the surface (M91:?, W = 0.2 mm)



h. Destannification (M91:222, W = 0.2 mm)

Figure 6.20 Different types of secondary metallic copper in Jin bronzes (W denotes width of the image)